arXiv:1705.03070v2 [cs.SY] 20 May 2017

A Multi-Class Dispatching and Charging Scheme for Autonomous Electric Mobility On-Demand

Syrine Belakaria*, Mustafa Ammous*, Sameh Sorour* and Ahmed Abdel-Rahim†‡
*Department of Electrical and Computer Engineering, University of Idaho, Moscow, ID, USA
†Department of Civil and Environmental Engineering, University of Idaho, Moscow, ID, USA
‡National Institute for Advanced Transportation Technologies, University of Idaho, Moscow, ID, USA
Email: {ammo1375, bela7898}@vandals.uidaho.edu, {samehsorour, ahmed}@uidaho.edu

***Abstract*—Despite the significant advances in vehicle automation and electrification, the next-decade aspirations for massive deployments of autonomous electric mobility on demand (AEMoD) services are still threatened by two major bottlenecks, namely the computational and charging delays. This paper proposes a solution for these two challenges by suggesting the use of fog computing for AEMoD systems, and developing an optimized multi-class charging and dispatching scheme for its vehicles. A queuing model representing the proposed multi-class charging and dispatching scheme is first introduced. The stability conditions of this model and the number of classes that fit the charging capabilities of any given city zone are then derived. Decisions on the proportions of each class vehicles to partially/fully charge, or directly serve customers are then optimized using a stochastic linear program that minimizes the maximum response time of the system. Results show the merits of our proposed model and optimized decision scheme compared to both the always-charge and the equal split schemes.**

***Keywords*—Autonomous Mobility On-Demand; Electric Vehicle; Fog-based Architecture; Dispatching; Charging; Queuing Systems.**

I. Introduction

Urban transportation systems are facing tremendous challenges nowadays due to the dominant dependency and massive increases on private vehicle ownership, which result in dramatic increases in road congestion, parking demand [1], increased travel times [2], and carbon footprint [3] [4]. These challenges have significantly can be mitigated with the significant advances and gradual maturity of vehicle electrification, automation, and wireless connectivity. With more than 10 million self-driving cars expected to be on the road by 2020 [5], it is strongly forecasted that vehicle ownership will significantly decline by 2025, as it will be replaced by the novel concept of Autonomous Electric Mobility on-Demand (AEMoD) services [6], [7]. In such system, customers will simply need to press some buttons on an app to promptly get an autonomous electric vehicle transporting them door-to-door, with no pick-up/drop-off and driving responsibilities, no dedicated parking needs, no carbon emission, no vehicle insurance and maintenance costs, and extra in-vehicle work/leisure times. With these qualities, AEMoD systems will significantly prevail in attracting millions of subscribers across the world and in providing on-demand and hassle-free private urban mobility.

Despite the great aspirations for wide AEMoD service deployments by early-to-mid next decade, the timeliness (and thus success) of such service is threatened by two major bottlenecks. First, the expected massive demand of AEMoD services will result in excessive if not prohibitive computational and communication delays if cloud based approaches are employed for the micro-operation of such systems. Moreover, the typical full-battery charging rates of electric vehicles will not be able to cope with the gigantic numbers of vehicles involved in these systems, thus resulting in instabilities and unbounded customer delays. Several recent works [9], [10] have addressed other important problems in autonomous mobility on-demand systems but none of them considered the computational architecture for a massive demand on such services, and the vehicle electrification and charging limitations.

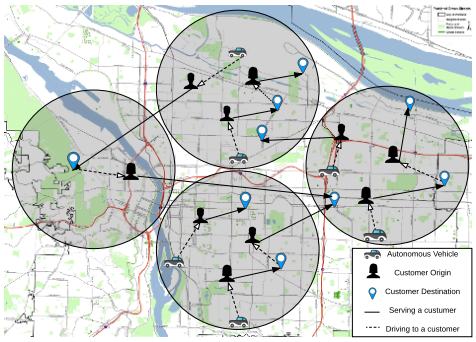


Fig. 1: Fog-based architecture for AEMoD system operation

In this paper, we suggest to solve the first problem by handling AEMoD system operations in a distributed fashion using fog computing [8]. Fog computing is a novel distributed edge computing architecture that pushes computational resources close to the end entities, to provide them with low latency analytics and optimization solutions. The use of fog computing is justified by the fact that many of the AEMoD operations (e.g., dispatching and charging) are localized. Indeed, vehicles located in any city zone are ones that can reach the customers in that zone within a limited time frame. They will also charge in near-by charging points within the zone. Fig.1 illustrates a candidate fog-based architecture that can support real-time micro-operational decisions (e.g, dispatching and charging) for AEMoD systems with extremely low computation and communications delays. The fog controller in each service zone is responsible of collecting information about customer requests, vehicle in-flow to the service zone, their state-of-charge (SoC), and the available full-battery charging rates in the service zone. Given the collected information, it can promptly make dispatching, and charging decisions for these vehicles in a timely manner.

One way to solve the second problem is to smartly cope with the available charging capabilities of each service zone, and efficiently manage the charging options of different SoC vehicles. This former solution can be achieved by introducing the option of partial vehicle charging instead of fully relying on full vehicle charging only when their batteries are depleted. To efficiently manage this partial charging scheme for different SoC vehicles, and motivated by the fact that different customers can be classified in ascending order of their required trip distances (and thus SoC of their allocated vehicles), this paper proposes a multi-class dispatching and charging system of AEMoD vehicles. Arriving vehicles in each service zone are subdivided into different classes in ascending order of their SoC corresponding to the different customer classes. Different proportions of each class vehicles will be then prompted by the fog controller to either wait (without charging) for dispatching to its corresponding customer class or partially charge to serve the subsequent customer class. Even vehicles arriving with depleted batteries will be allowed to either partially or fully charge to serve the first or last class customers, respectively.

The question now is: *What is the optimal proportion of vehicles from each class to dispatch or partially/fully charge, to both maintain charging stability and minimize the maximum response time of the system?* To address this question, a queuing model representing the proposed multi-class charging and dispatching scheme is first introduced. The stability conditions of this model and the number of classes that fit the charging capabilities of the service zone are then derived. Decisions on the proportions of each class vehicles to partially/fully charge, or directly serve customers are then optimized using a stochastic linear program that minimizes the maximum response time of the system. Finally, the merits of our proposed optimized decision scheme are tested and compared to both the always-charge and the equal split schemes.

II. System Model

We consider one service zone controlled by a fog controller connected to: (1) the service request apps of cutomers in the zone; (2) the AEMoD vehicles; (3) C rapid charging points distributed in the service zone and designed for short-term partial charging; and (4) one spacious rapid charging station designed for long-term full charging. AEMoD vehicles enter the service in this zone after dropping off their latest customers in it. Their detection as free vehicles by the zone's controller can thus be modeled as a Poisson process with rate λ_v. Customers request service from the system according to a Poisson process. Both customers and vehicles are classified into n classes based on an ascending order of their required trip distance and the corresponding SoC to cover this distance, respectively. From the thinning property of Poisson processes, the arrival process of Class i customers and vehicles, $i \in \{0, \dots, n\}$, are both independent Poisson processes with rates $\lambda_c^{(i)}$ and $\lambda_v p_i$, where p_i is the probability that the SoC of an arriving vehicle to the system belongs to Class i. Note that p_0 is the probability that a vehicle arrive with a depleted battery, and is thus not able to serve immediately. Consequently, $\lambda_c^{(0)} = 0$ as no customer will request a vehicle that cannot travel any distance. On the other hand, p_n is also equal to 0, because no vehicle can arrive to the system fully charged as it has just finished a prior trip.

Upon arrival, each vehicle of Class i, $i \in \{1, \dots, n-1\}$, will park anywhere in the zone until it is called by the fog controller to either: (1) serve a customer from Class i with probability q_i; or (2) partially charge up to the SoC of Class $i+1$ at any of the C charging points (whenever any of them becomes free), with probability $\overline{q}_i = 1 - q_i$, before parking again in waiting to serve a customer from Class $i+1$. As for Class 0 vehicles that are incapable of serving before charging, they will be directed to either fully charge at the central charging station with probability q_0, or partially charge at one of C charging points with probability $\overline{q}_0 = 1 - q_0$. In the former and latter cases, the vehicle after charging will wait to serve customers of Class n and 1, respectively.

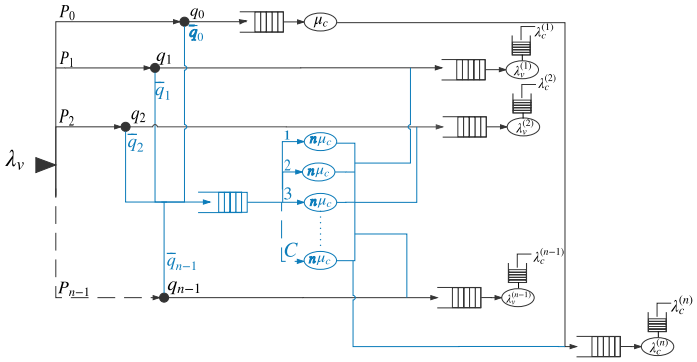


Fig. 2: Joint dispatching and partially/fully charging model, abstracting an AEMoD system in one service zone.

As widely used in the literature (e.g., [11], [12]), the full charging time of a vehicle with a depleted battery is assumed to be exponentially distributed with rate μ_c. Given uniform SoC quantization among the n vehicle classes, the partial charging time can then be modeled as an exponential random variable with rate $n\mu_c$. Note that the larger rate of the partial charging process is not due to a speed-up in the charging process but rather due to the reduced time of partially charging. The customers belonging to Class i, arriving at rate $\lambda_c^{(i)}$, will be served at a rate of $\lambda_v^{(i)}$, which includes the arrival rate of vehicles that: (1) arrived to the zone with a SoC belonging to Class i and were directed to wait to serve Class i customers; or (2) arrived to the zone with a SoC belonging to Class $i-1$ and were directed to partially charge to be able to serve Class i customers.

Given the above description and modeling of variables, the entire zone dynamics can thus be modeled by the queuing system depicted in Fig.2. This system includes n M/M/1 queues for the n classes of customer service, one M/M/1 queue for the charging station, and one M/M/C queue representing the partial charging process at the C charging points.

Assuming that the service zones will be designed to guarantee a maximum time for a vehicle to reach a customer, our goal in this paper is to minimize the maximum expected response time of the entire system. By response time, we mean the time elapsed between the instant when an arbitrary customer requests a vehicle, and the instant when a vehicle starts moving from its parking or charging spot towards this customer.

III. System Stability Conditions

In this section, we first deduce the stability conditions of our proposed joint dispatching and charging system, using the basic laws of queuing theory. We will also derive an expression

for the lower bound on the number n of needed classes that fit the charging capabilities of any arbitrary service zone. Each of the n classes of customers are served by a separate queue of vehicles, with $\lambda_v^{(i)}$ being the arrival rate of the vehicles that are available to serve the customers of the i^{th} class. Consequently, it is the service rate of the customers i^{th} arrival queues. We can thus deduce from Fig. 2 and the system model in the previous section that :

$$\begin{aligned} \lambda_v^{(i)} &= \lambda_v(p_{i-1}\overline{q}_{i-1} + p_i q_i),\ i = 1, \ldots, n-1. \\ \lambda_v^{(n)} &= \lambda_v(p_{n-1}\overline{q}_{n-1} + p_0 q_0) \end{aligned} \tag{1}$$

Since we know that $\overline{q}_i + q_i = 1$ Then we substitute $\overline{q}_i$ by $1 - q_i$ in order to have a system with n variables

$$\begin{aligned} \lambda_v^{(i)} &= \lambda_v(p_{i-1} - p_{i-1}q_{i-1} + p_i q_i),\ i = 1, \ldots, n-1 \\ \lambda_v^{(n)} &= \lambda_v(p_{n-1} - p_{n-1}q_{n-1} + p_0 q_0) \end{aligned} \tag{2}$$

From the well-known stability condition of an M/M/1 queue, we have:

$$\lambda_v^{(i)} > \lambda_c^{(i)},\ i = 1, \ldots, n \tag{3}$$

Before reaching the customer service queues, the vehicles will go through a decision step of either to go to these queues immediately or partially charge. The stability of the charging queues should be guaranteed in order to ensure the global stability of the entire system at the steady state. From the model described in the previous section, and by the well-known stability conditions of M/M/C and M/M/1 queues, we have the following stability constraints on the C charging points and central charging station queues, respectively:

$$\begin{aligned} &\sum_{i=0}^{n-1} \lambda_v(p_i - p_i q_i) < C(n\mu_c) \\ &\lambda_v p_0 q_0 < \mu_c \end{aligned} \tag{4}$$

The following lemma allows the estimation of the average needed in-flow rate of vehicles for a given service zone given its rate of customer demand on AEMoD services.

Lemma 1: For the entire system stability, the total arrival rate of the customers belonging to all the classes should be strictly less than the total arrival rate of the vehicles

$$\sum_{i=1}^{n} \lambda_c^{(i)} < \lambda_v \tag{5}$$

Proof: The proof of Lemma 1 is in Appendix A. ■

Furthermore, the following lemma establishes a lower bound on the number of classes n, given the arrival rate of the vehicles λ_v, the full charging rate μ_c, and the number C of partial charging points.

Lemma 2: For stability of the charging queues, the number of classes n is the system must obey the following inequality:

$$n > \frac{\lambda_v}{C\mu_c} - \frac{1}{C} \tag{6}$$

Proof: The proof of Lemma 2 is in Appendix B. ■

IV. Joint Charging and Dispatching optimization

A. Problem Formulation

The goal of this paper is to minimize the maximum expected response time of the system's classes. The response time of any class is defined as the average of the duration between any customer putting a request until a vehicle is dispatched to serve him/her. The maximum expected response time of the system can be expressed as:

$$\max_{i \in \{1,\ldots,n\}} \left\{ \frac{1}{\lambda_v^{(i)} - \lambda_c^{(i)}} \right\} \tag{7}$$

It is obvious that the system's class having the maximum expected response time is the one that have the minimum expected response rate. In other words, we have:

$$\arg \max_{i \in \{1,\ldots,n\}} \left\{ \frac{1}{\lambda_v^{(i)} - \lambda_c^{(i)}} \right\} = \arg \min_{i \in \{1,\ldots,n\}} \left\{ \lambda_v^{(i)} - \lambda_c^{(i)} \right\} \tag{8}$$

. Consequently, minimizing the maximum expected response time is equivalent to maximizing the minimum expected response rate. Using the epigraph form [13] of the latter problem, we get the following stochastic optimization problem:

$$\underset{q_0, q_1, \ldots, q_{n-1}}{\text{maximize}}\ R \tag{9a}$$

s.t

$$\lambda_v(p_{i-1} - p_{i-1}q_{i-1} + p_i q_i) - \lambda_c^{(i)} \geq R,\ i = 1, \ldots, n-1 \tag{9b}$$

$$\lambda_v(p_{n-1} - p_{n-1}q_{n-1} + p_0 q_0) - \lambda_c^{(n)} \geq R \tag{9c}$$

$$\sum_{i=0}^{n-1} \lambda_v(p_i - p_i q_i) < C(n\mu_c) \tag{9d}$$

$$\lambda_v p_0 q_0 < \mu_c \tag{9e}$$

$$\sum_{i=0}^{n-1} p_i = 1,\ 0 \leq p_i \leq 1,\ i = 0, \ldots, n-1 \tag{9f}$$

$$0 \leq q_i \leq 1,\ i = 0, \ldots, n-1 \tag{9g}$$

$$R > 0 \tag{9h}$$

The n constraints in (9b) and (9c) represent the epigraph form's constraints on the original objective function in the right hand side of (8), after separation [13] and substituting every $\lambda_v^{(i)}$ by its expansion form in (2). The constraints in (9d) and (9e) represent the stability conditions on charging queues. The constraints in (9f) and (9g) are the axiomatic constraints on probabilities (i.e., values being between 0 and 1, and sum equal to 1). Finally, Constraint (9h) is a positivity constraint on the minimum expected response rate. Clearly, the above equation is a linear program with linear constraints, which can be solved analytically using convex optimization analysis. This will be the target of the next subsection.

B. Optimal Dispatching and Charging Decisions

The problem in (9) is a convex optimization problem with differentiable objective and constraint functions that satisfies Slater's condition. Consequently, the KKT conditions provide necessary and sufficient conditions for optimality. Therefore, applying the KKT conditions to the constraints of the problem and the gradient of the Lagrangian function allows us to find

the analytical solution of the decisions q_i. The Lagrangian function associated with the optimization problem in (9) is given by the following expression:

$$\begin{aligned} L(\mathbf{q}, R, \boldsymbol{\alpha}, \boldsymbol{\beta}, \boldsymbol{\gamma}, \boldsymbol{\omega}) &= -R + \sum_{i=1}^{n-1} \alpha_i(\lambda_v(p_{i-1}q_{i-1} - p_i q_i) \\ &+ R - \lambda_v p_{i-1} + \lambda_c^{(i)}) + \alpha_n(\lambda_v(p_{n-1}q_{n-1} - p_0 q_0) \\ &+ R - \lambda_v p_{n-1} + \lambda_c^{(n)}) + \beta_0(\sum_{i=0}^{n-1} \lambda_v(p_i - p_i q_i) - C(n\mu_c)) \\ &+ \beta_1(\lambda_v p_0 q_0 - \mu_c) + \sum_{i=0}^{n-1} \gamma_i(q_i - 1) - \sum_{i=0}^{n-1} \omega_i q_i + \omega_n R \,, \end{aligned} \tag{10}$$

where $\mathbf{q}$ is the vector of dispatching decisions (i.e. $\mathbf{q} = [q_0, \ldots, q_{n-1}]$), and where:

- $\boldsymbol{\alpha} = [\alpha_i]$, such that α_i is the associated Lagrange multiplier to the i-th customer queues inequality.
- $\boldsymbol{\beta} = [\beta_i]$, such that βi is the associated Lagrange multiplier to the i-th charging queues inequality.
- $\boldsymbol{\gamma} = [\gamma_i]$, such that γ_i is the associated Lagrange multiplier to the i-th upper bound inequality.
- $\boldsymbol{\omega} = [\omega_i]$, such that ω_i is the associated Lagrange multiplier to the i-th lower bound inequality.

By applying the KKT conditions on the equality and inequality constraints, the following theorem illustrates the optimal solution of the problem in (9)

Theorem 1: The optimal charging/dispatching decisions of the optimization problem in (9) can be expressed as follows:

$$\begin{aligned} q_0^* &= \begin{cases} 0 & \alpha_1^* > \alpha_n^* \\ 1 & \alpha_1^* < \alpha_n^* \end{cases} \\ q_i^* &= \begin{cases} 0 & \alpha_{i+1}^* > \alpha_i^* \\ 1 & \alpha_{i+1}^* < \alpha_i^* \end{cases}, \; i = 1, \ldots, n-1. \\ &\text{if } \alpha_1^* = \alpha_n^* \neq 0 \begin{cases} q_1^* = \frac{p_0 q_0^*}{p_1} - \frac{\lambda_v p_0 - \lambda_c^{(1)} - R^*}{\lambda_v p_1} \\ q_{n-1}^* = \frac{p_0 q_0^*}{p_{n-1}} - \frac{\lambda_v p_0 - \lambda_c^{(n)} - R^*}{\lambda_v p_{n-1}} \end{cases} \\ &\text{if } \alpha_{i+1}^* = \alpha_i^* \neq 0 \begin{cases} q_i^* = \frac{p_{i-1} q_{i-1}^*}{p_i} - \frac{\lambda_v p_{i-1} - \lambda_c^{(i)} - R^*}{\lambda_v p_i} \\ q_{i+1}^* = \frac{p_i q_i^*}{p_{i+1}} - \frac{\lambda_v p_i - \lambda_c^{(i+1)} - R^*}{\lambda_v p_{i+1}} \end{cases} \\ &i = 1, \ldots, n-1. \end{aligned} \tag{11}$$

Proof: The proof of Theorem 1 is in Appendix C. ■

C. Maximum Expected Response Time

Again, since the problem in (9) is convex with convex with differentiable objective and constraint functions, then strong duality holds, which implies that the solution to the primal and dual problems are identical. By solving the dual problem, we can express the optimal value of the maximum expected response time as the reciprocal of the minimum expected response rate of the system, which is introduced in the following theorem.

Theorem 2: The minimum expected response rate R^* of the entire system can be expressed as:

$$R^* = \sum_{i=1}^{n} \left(\lambda_v p_{i-1} - \lambda_c^{(i)}\right) \alpha_i^* + \sum_{i=0}^{n-1} \gamma_i^* \tag{12}$$

Proof: The proof of Theorem 2 is in Appendix D. ■

V. Simulation Results

In this section, we test the merits of our proposed scheme using extensive simulations. The simulation metrics used to evaluate these merits are the maximum and average expected response times of the different classes. For all the performed simulation figures, the full-charging rate of a vehicle is set to $\mu_c = 0.033$ mins^{-1}, and the number of charging points $C = 40$.

Fig. 3 illustrates both the interplay of λ_v and $\sum_{i=1}^{n} \lambda_c^{(i)}$, established in Lemma 1, and effect of increasing the number of classes n beyond its strict lower bound introduced in Lemma 2.Fig. 3 depict the maximum and average expected response time for different values of $\sum_{i=1}^{n} \lambda_c^{(i)}$, while fixing λ_v to 15 min^{-1}. For this setting, $n = 12$ is the smallest number of classes that satisfy the stability condition in Lemma 2.

It is easy to notice that the response times for all values of n increase dramatically when the $\sum_{i=1}^{n} \lambda_c^{(i)}$ approaches λ_v. Moreover, it shows clearly that increasing n beyond its stability lower bound increases both the maximum and average response times. We thus conclude that the optimal number of classes is the smallest value satisfying Lemma 2:

$$n^* = \begin{cases} \frac{\lambda_v}{C\mu_c} - \frac{1}{C} + 1 & \frac{\lambda_v}{C\mu_c} - \frac{1}{C} \text{ integer} \\ \left\lceil \frac{\lambda_v}{C\mu_c} - \frac{1}{C} \right\rceil & \text{Otherwise} \end{cases} \tag{13}$$

Fig. 4 depicts the expected response time performances for different distributions of the vehicle SoC and customer trip distances. In this study, we fix $\lambda_v = 8$ and thus $n = 7$. We can infer from the figure that the response times for Gaussian distributions of trip distances and both Gaussian or decreasing ones for SoCs are the lowest and exhibit the least response time variance. Luckily, these are the most realistic distributions for both variables. This is justified by the fact that vehicles arrive to the system after trips of different distances, which makes their SoC either Gaussian or slightly decreasing. Likewise, customers requiring mid-size distances are usually more than those requiring very small and very long distances.

Fig. 5 compares the expected response time performances against $\sum_{i=1}^{n} \lambda_c^{(i)}$, for different decision approaches, namely our derived optimal decisions, always partially charge decisions (i.e. $q_i = 1 \; \forall \; i$) and equal split decisions (i.e. $q_i = 0.5 \; \forall \; i$), for $\lambda_v = 8$ and thus $n = 7$. These two schemes represent non-optimized policies, in which each vehicle takes its own fixed decision irrespective of the system parameters. The figure clearly shows superior maximum and average performances for our derived optimal policy compared to the other two policies, especially as $\sum_{i=1}^{n} \lambda_c^{(i)}$ gets closer to λ_v, which are the most properly engineerd sceanrios (as large differences between these two quantities results in very low utilization). Gains of 13.3% and 21.3% on the average and maximum performances can be noticed compared to the always charge policy. This shows the importance of our proposed scheme in achieving better customer satisfaction.

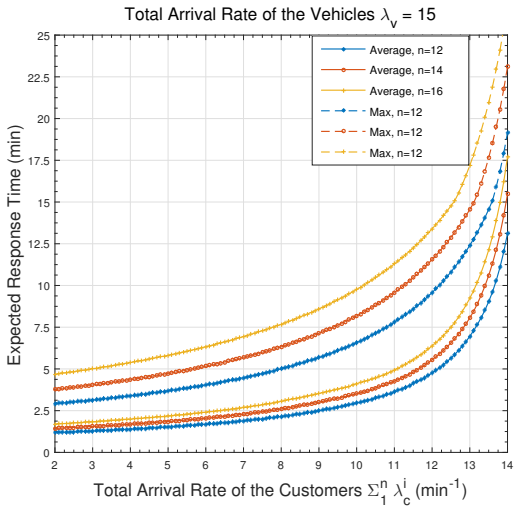


Fig. 3: Expected response times for different $\sum_{i=1}^{n} \lambda_c^{(i)}$

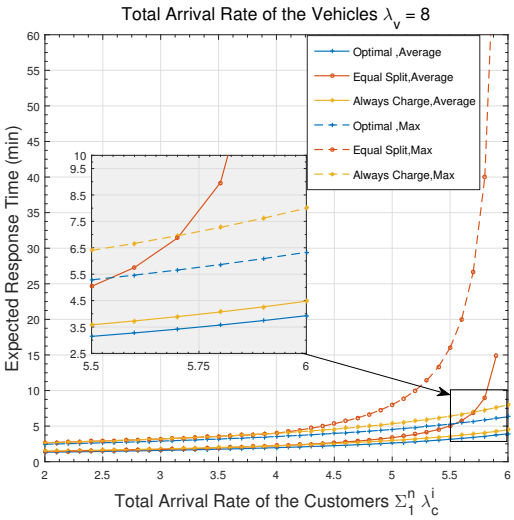


Fig. 5: Comparison to non-optimized policies.

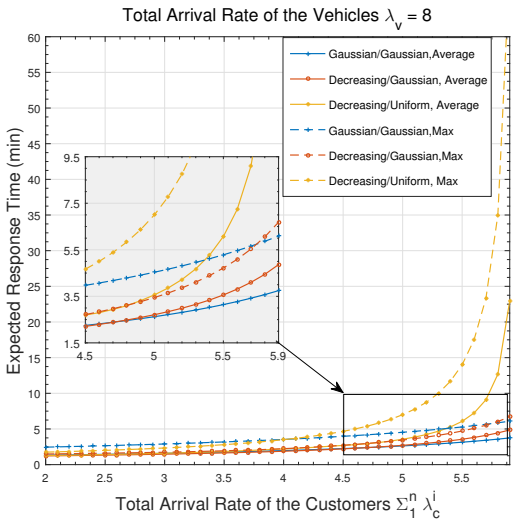


Fig. 4: Effect of different customer and SoC distributions.

VI. Conclusion

In this paper, we proposed solutions to the computational and charging bottlenecks threatening the success of AEMoD systems. The computational bottleneck can be resolved by employing a fog-based architecture to distribute the optimization loads over different service zones, reduce communication delays, and matches the nature of dispatching and charging processes of AEMoD vehicles. We also proposed a multi-class dispatching and charging scheme and developed its queuing model and stability conditions. We then formulated the problem of optimizing the proportions of vehicles of each class that will partially/fully charge or directly serve customers as a stochastic linear program, in order to minimize the maximum expected system response time while respecting the system stability constraints. The optimal decisions and corresponding maximum response time were analytically derived. The optimal number of classes both minimizing the response time and matching the vehicle and charging statistics was also characterized. Simulation results demonstrated both the merits of our proposed optimal decision scheme compared to typical non-optimized schemes, and its performance for different distributions of vehicle SoC and customer trip distances.

References

[1] W. J. Mitchell, C. E. Borroni-Bird, and L. D. Burns, "Reinventing the Automobile: Personal Urban Mobility for the 21st Century". Cambridge, MA: The MIT Press, 2010.

[2] D. Schrank, B. Eisele, and T. Lomax, "TTIs 2012 Urban Mobility Report," *Texas A&M Transportation Institute*, Texas, USA.2012.

[3] U. N. E. Programme, "The Emissions Gap Report 2013 - UNEP," *Tech. Rep.*, 2013.

[4] U. E. P. Agency, "Greenhouse Gas Equivalencies Calculator," *Tech.Rep.*, 2014. [Online]: http://www.epa.gov/cleanenergy/energy-resources/refs.html

[5] "IoT And Smart Cars: Changing The World For The Better," *Digitalist Magazine*, August 30, 2016. [Online]: http://www.digitalistmag.com/iot/2016/08/30/iot-smart-connected-cars-willchange-world-04422640

[6] "Transportation Outlook: 2025 to 2050," *Navigant Research, Q216*, 2016. [Online]: http://www.navigantresearch.com/research/transportation-outlook-2025-to-2050.

[7] "The Future Is Now: Smart Cars And IoT In Cities," *Forbes*, June 13, 2016. [Online]: http://www.forbes.com/sites/pikeresearch/2016/06/13/the-future-is-now-smartcars/63c0a25248c9

[8] "Fog Computing and the Internet of Things: Extend the Cloud to Where the Things Are," *Cisco White Paper*, 2015. [Online]:http://www.cisco.com/c/dam/en_us/solutions/trends/iot/docs/computing-overview.pdf

[9] R. Zhang, K. Spieser, E. Frazzoli, and M. Pavone, "Models, Algorithms, and Evaluation for Autonomous Mobility-On-Demand Systems," *in Proc. of American Control Conf.*, Chicago, Illinois, 2015.

[10] R. Zhang, F. Rossi, and M. Pavone, "Model Predictive Control of Autonomous Mobility-on-Demand Systems," *in Proc. IEEE Conf. on Robotics and Automation*, Stockholm, Sweden, 2016.

[11] H. Liang, I. Sharma, W. Zhuang, and K. Bhattacharya,"Plug-in Electric Vehicle Charging Demand Estimation based on Queueing Network Analysis," *IEEE Power and Energy Society General Meeting*, 2014.

[12] K. Zhang, Y. Mao, S. Leng, Y. Zhang, S. Gjessing, and D.H.K. Tsang, "Platoon-based Electric Vehicles Charging with Renewable Energy Supply: A Queuing Analytical Model," *in Proc. of IEEE International Conference on Communications (ICC16)*, 2016.

[13] S. Boyd and L. Vandenberghe, "Convex Optimization", 1st ed. *Cambridge: Cambridge University Press*, 2015.

APPENDIX A
PROOF OF LEMMA 1

From (2) and (3) we have :

$$\begin{aligned} &\lambda_c^{(i)} < \lambda_v(p_{i-1}\overline{q}_{i-1} + p_i q_i),\ i = 1, \ldots, n-1. \\ &\lambda_c^{(n)} < \lambda_v(p_{n-1}\overline{q}_{n-1} + p_0 q_0),\ i = n \end{aligned} \tag{14}$$

The summation of all the inequalities in (14) gives a new inequality

$$\sum_{i=1}^{n} \lambda_c^{(i)} < \lambda_v[\sum_{i=1}^{n-1} (p_{i-1}\overline{q}_{i-1} + p_i q_i) + (p_{n-1}\overline{q}_{n-1} + p_0 q_0)] \tag{15}$$

$$\sum_{i=1}^{n} \lambda_c^{(i)} < \lambda_v[p_0\overline{q}_0 + p_1 q_1 + p_1\overline{q}_1 + ... + p_{n-1}\overline{q}_{n-1} + p_0 q_0] \tag{16}$$

We have $\overline{q}_i + q_i$ so $p_i\overline{q}_i + p_i q_i = p_i$

$$\sum_{i=1}^{n} \lambda_c^{(i)} < \lambda_v(p_0 + p_1 + p_2 + ... + p_{n-1}) \tag{17}$$

We have $\sum_{i=0}^{n-1} p_i = 1$ so $\sum_{i=1}^{n} \lambda_c^{(i)} < \lambda_v$

APPENDIX B
PROOF OF LEMMA 2

The summation of the inequalities given by (4) $\forall\ i = \{0, \ldots, n\}$ gives the following inequality :

$$\lambda_v \sum_{i=0}^{n-1} p_i - \lambda_v \sum_{i=0}^{n-1} p_i q_i + \lambda_v p_0 q_0 < C(n\mu_c) + \mu_c \tag{18}$$

Since $\sum_{i=0}^{n-1} p_i = 1$ (because $p_n = 0$ as described in Section 2), we get:

$$\lambda_v - \lambda_v \sum_{i=1}^{n-1} p_i q_i < \mu_c(Cn + 1) \tag{19}$$

In the worst case, all the vehicles will be directed to partially charge before serving, which means that always $q_i = 0$. Therefore, we get:

$$Cn > \frac{\lambda_v}{\mu_c} - 1\ , \tag{20}$$

which can be re-arranged to be:

$$n > \frac{\lambda_v}{C\mu_c} - \frac{1}{C} \tag{21}$$

APPENDIX C
PROOF OF THEOREM 1

Applying the KKT conditions to the inequalities constraints of (9), we get:

$$\begin{aligned} &\alpha_i^*(\lambda_v(p_{i-1}q_{i-1}^* - p_i q_i^*) + R^* - \lambda_v p_{i-1} + \lambda_c^{(i)}) = 0 \\ &i = 1, \ldots, n-1. \\ &\alpha_n^*(\lambda_v(p_{n-1}q_{n-1}^* - p_0 q_0^*) + R^* - \lambda_v p_{n-1} + \lambda_c^{(n)}) = 0. \\ &\beta_0^*(\sum_{i=0}^{n-1} \lambda_v(p_i - p_i q_i^*) - C(n\mu_c)) = 0. \\ &\beta_1^*(\lambda_v p_0 q_0^* - \mu_c) = 0 \\ &\gamma_i^*(q_i^* - 1) = 0,\ i = 0, \ldots, n-1. \\ &\omega_i^* q_i^* = 0,\ i = 0, \ldots, n-1. \\ &\omega_n^* R^* = 0. \end{aligned} \tag{22}$$

Likewise, applying the KKT conditions to the Lagrangian function in (10), and knowing that the gradient of the Lagrangian function goes to 0 at the optimal solution, we get the following set of equalities:

$$\begin{aligned} &\lambda_v p_i(\alpha_{i+1}^* - \alpha_i^*) = \omega_i^* - \gamma_i^*,\ i = 1, \ldots, n-1. \\ &\lambda_v p_0(\alpha_1^* - \alpha_n^*) = \omega_0^* - \gamma_0^* \\ &\sum_{i=1}^{n-1} \alpha_i^* = 1 \end{aligned} \tag{23}$$

From Burke's theorem on the stability condition of the queues, the constraints on the charging queues are strict inequalities and the constraints on R should also be strictly larger than 0. Combining the Burke's theorem and the equations on (22), we find that all the $\beta_0^* = \beta_1^* = 0$ and $\omega_n^* = 0$.

Knowing that the gradient of the Lagrangian goes to 0 at the optimal solutions, we get the system of equalities given by (23). The fact that $\beta_i^* = 0$ and $\omega_n^* = 0$ explains the absence of β_i^* and ω_n^* in (11) The result given by multiplying the first equality in (23) by q_i^* and the second equality by q_0^* combined with the last three equalities given by (22) gives :

$$\begin{aligned} &\lambda_v p_i(\alpha_{i+1}^* - \alpha_i^*)q_i^* = -\gamma_i^*,\ i = 1, \ldots, n-1. \\ &\lambda_v p_0(\alpha_1^* - \alpha_n^*)q_0^* = -\gamma_0^* \\ &\sum_{i=1}^{n-1} \alpha_i^* = 1 \end{aligned} \tag{24}$$

(24) Inserted in the fifth equality in (22) gives :

$$\begin{aligned} &\lambda_v p_i(\alpha_{i+1}^* - \alpha_i^*)(q_i^* - 1)q_i^* = 0,\ i = 1, \ldots, n-1. \\ &\lambda_v p_0(\alpha_1^* - \alpha_n^*)(q_0^* - 1)q_0^* = 0 \\ &\sum_{i=1}^{n-1} \alpha_i^* = 1 \end{aligned} \tag{25}$$

From (25) we have $0 < q_0^* < 1$ only if $\alpha_1^* = \alpha_n^*$ And $0 < q_i^* < 1$ only if $\alpha_{i+1}^* = \alpha_i^*$ Since $0 \leq q_i^* \leq 1$ then these equalities may not always be true

if $\alpha_1^* > \alpha_n^*$ and we know that $\gamma_0^* \geq 0$ then $\gamma_0^* = 0$ which gives $q_0^* \neq 1$ and $q_0^* = 0$.

if $\alpha_{i+1}^* > \alpha_i^*$ and we know that $\gamma_i^* \geq 0$ then $\gamma_i^* = 0$ which gives $q_i^* \neq 1$ and $q_i^* = 0$

if $\alpha_1^* < \alpha_n^*$ then $\gamma_0^* > 0$ (it cannot be 0 because this will

contradict with the value of q_i), which implies that $q_0^* = 1$.

if $\alpha_{i+1}^* < \alpha_i^*$ then $\gamma_i^* > 0$ (it cannot be 0 because this contradicts with the value of q_i), which implies that $q_i^* = 1$

Otherwise , if $\alpha_1^* = \alpha_n^* \neq 0$ (they cannot be equal to 0 at the same time, which means that $q_0 = 1$, and we know in advance that this cannot be the case here), we have $q_1^* = \frac{p_0 q_0^*}{p_1} - \frac{\lambda_v p_0 - \lambda_c^{(1)} - R^*}{\lambda_v p_1}$ and $q_{n-1}^* = \frac{p_0 q_0^*}{p_{n-1}} - \frac{\lambda_v p_0 - \lambda_c^{(n)} - R^*}{\lambda_v p_{n-1}}$

Finally, if $\alpha_{i+1}^* = \alpha_i^* \neq 0$ (they cannot be equal to 0 at the same time, which means that $q_i = 1$, and we know in advance that this cannot be the case here), we have $q_i^* = \frac{p_{i-1} q_{i-1}^*}{p_i} - \frac{\lambda_v p_{i-1} - \lambda_c^{(i)} - R^*}{\lambda_v p_i}$ and $q_{i+1}^* = \frac{p_i q_i^*}{p_{i+1}} - \frac{\lambda_v p_i - \lambda_c^{(i+1)} - R^*}{\lambda_v p_{i+1}}$

APPENDIX D
PROOF OF THEOREM 2

To prove this theorem, we first start by putting the problem on the standard linear programming form as follows:

$$
\begin{aligned}
&\underset{q_0, q_1, \ldots, q_{n-1}}{\text{minimize}} \quad -R \\
&\text{subject to} \\
&\text{Constraint on costumers arrivals queues} \\
&\lambda_v(p_{i-1}q_{i-1} - p_i q_i) + R \leq \lambda_v p_{i-1} - \lambda_c^{(i)},\ i = 1, \ldots, n-1. \\
&\lambda_v(p_{n-1}q_{n-1} - p_0 q_0) + R \leq \lambda_v p_{n-1} - \lambda_c^{(n)}. \\
&\text{Constraint on charging vehicles queues} \\
&-\lambda_v \sum_{i=0}^{n-1} p_i q_i^* < C(n\mu_c) - \lambda_v \\
&\lambda_v p_0 q_0 < \mu_c \\
&\text{Constraint on probabilities and decisions} \\
&q_i \leq 1,\ i = 0, \ldots, n-1. \\
&-q_i \leq 0,\ i = 0, \ldots, n-1. \\
&-R < 0. \\
&\sum_{i=0}^{n-1} p_i = 1,\ 0 < p_i < 1,\ i = 0, \ldots, n-1.
\end{aligned}
\tag{26}
$$

Writing the problem on its matrix form, we get:

$$
\begin{aligned}
&\underset{X}{\text{minimize}} \quad \mathbf{c}^T \mathbf{x} \\
&\text{subject to} \quad \mathbf{A}\mathbf{x} \preceq \mathbf{b}
\end{aligned}
\tag{27}
$$

where:

$$
\mathbf{x}_{(n+1\times 1)} = \begin{pmatrix} q_0 \\ q_1 \\ \vdots \\ q_{n-1} \\ R \end{pmatrix} \qquad \mathbf{c}_{(n+1\times 1)} = \begin{pmatrix} 0 \\ 0 \\ 0 \\ \vdots \\ -1 \end{pmatrix}
$$

$$
\mathbf{b}_{(3n+4\times 1)} = \begin{pmatrix} \lambda_v p_0 - \lambda_c^{(1)} \\ \vdots \\ \lambda_v p_{n-1} - \lambda_c^{(n)} \\ C(n\mu_c) - \lambda_v \\ \mu_c \\ 1 \\ \vdots \\ 1 \\ \infty \\ 0 \\ \vdots \\ 0 \end{pmatrix}
\tag{28}
$$

$$
\mathbf{A}_{(3n+4\times n+1)} = \begin{pmatrix}
\lambda_v p_0 & -\lambda_v p_1 & 0 & \ldots & 0 & 1 \\
0 & \lambda_v p_1 & -\lambda_v p_2 & \ldots & 0 & 1 \\
\vdots & \ddots & \ddots & \ddots & \ddots & \vdots \\
0 & \ldots & 0 & \lambda_v p_{n-2} & -\lambda_v p_{n-1} & 1 \\
-\lambda_v p_0 & 0 & \ldots & \ldots & \lambda_v p_{n-1} & 1 \\
-\lambda_v p_0 & -\lambda_v p_1 & \ldots & \ldots & -\lambda_v p_{n-1} & 0 \\
\lambda_v p_0 & 0 & \ldots & \ldots & \ldots & 0 \\
\multicolumn{6}{c}{I_{n+1}} \\
\multicolumn{6}{c}{-I_{n+1}}
\end{pmatrix}
\tag{29}
$$

The matrix form of the Lagrangian function can be thus expressed as: Lagrangian :

$$
L(\mathbf{x}, \boldsymbol{\nu}) = \mathbf{c}^T \mathbf{x} + \boldsymbol{\nu}^T (\mathbf{A}\mathbf{x} - \mathbf{b}) = -\mathbf{b}^T + (\mathbf{A}^T \boldsymbol{\nu} + \mathbf{c})^T \mathbf{x}\,, \tag{30}
$$

where $\boldsymbol{\nu}$ is the vector of the dual variables or Lagrange multipliers vector associated with the problem 27. Each element ν_i of $\boldsymbol{\nu}$ is the Lagrange multiplier associated with the i-th inequality constraint $\mathbf{a}_i \mathbf{x} - b_i \leq 0$, where $\mathbf{a}_i$ and b_i are the the i-th row and and i-th element of matrix $\mathbf{A}$ and vector $\mathbf{b}$, respectively. In fact $\boldsymbol{\nu}$ is the vector that includes all the vectors $\boldsymbol{\alpha}$, $\boldsymbol{\beta}$, $\boldsymbol{\gamma}$, $\boldsymbol{\omega}$ as follows:

$$
\boldsymbol{\nu}^T_{(1\times 3n+4)} = (\alpha_1\ \ldots\ \alpha_n\ \beta_0\ \beta_1\ \gamma_0\ \ldots\ \gamma_n\ \omega_0\ \ldots\ \omega_n) \tag{31}
$$

We will used this combined notation for ease and clarity of notation.

The Lagrange dual function is expressed as:

$$
g(\boldsymbol{\nu}) = \inf_{\mathbf{x}}\ L(\mathbf{x}, \boldsymbol{\nu}) = -\mathbf{b}^T \boldsymbol{\nu} + \inf_{\mathbf{x}}\ (\mathbf{A}^T \boldsymbol{\nu} + \mathbf{c})^T \mathbf{x}\,, \tag{32}
$$

The solution for this function is easily determined analytically, since a linear function is bounded below only when it is identically zero. Thus, $g(\boldsymbol{\nu}) = -\infty$ except when $\mathbf{A}^T \boldsymbol{\nu} + \mathbf{c} = \mathbf{0}$,

where $\mathbf{0}$ is the all zero vector. Consequently, we have:

$$g(\boldsymbol{\nu}) = \begin{cases} -\mathbf{b}^T\boldsymbol{\nu} & \mathbf{A}^T\boldsymbol{\nu} + \mathbf{c} = \mathbf{0} \\ -\infty & \text{ortherwise} \end{cases} \tag{33}$$

For each $\nu \succeq \mathbf{0}$ (i.e., $\nu_i \geq 0 \ \forall \ i$), the Lagrange dual function gives us a lower bound on the optimal value of the original optimization problem. This leads to a new equivalent optimization problem, which is the dual problem:

$$\begin{aligned} \underset{\boldsymbol{\nu}}{\text{maximize}} \quad & g(\boldsymbol{\nu}) = -\mathbf{b}^T\boldsymbol{\nu} \\ \text{subject to} \quad & \mathbf{A}^T\boldsymbol{\nu} + \mathbf{c} = \mathbf{0} \\ & \boldsymbol{\nu} \succeq \mathbf{0} \end{aligned} \tag{34}$$

Applying Slater's Theorem for duality qualification, and since strong duality holds for the considered optimization problem, then solving the dual problem gives the exact optimal solution for the primal problem. This is described by the equality :

$$g(\boldsymbol{\nu}^*) = -\mathbf{b}^T\boldsymbol{\nu}^* = \mathbf{c}^T\mathbf{x}^* = -R^* \tag{35}$$

By expanding on the values of $\mathbf{b}$ and $\boldsymbol{\nu}$ in the above equation, the optimal value of R^* can be expressed as:

$$R^* = \sum_{i=1}^{n}(\lambda_v p_{i-1} - \lambda_c^{(i)})\alpha_i^* + \sum_{i=0}^{n-1}\gamma_i^* \tag{36}$$